Article

Discovery Medicine 2025; 37(201): 2439–2454
https://doi.org/10.24976/Discov.Med.202537201.206

The Role and Underlying Mechanism of the MCP-1/CCR2 Signaling Pathway in the Inflammatory Response of Atopic Dermatitis Pathogenesis

Jieyu Chen[1], Mian Xu[2,*]

[1]Department of Dermatology, The People's Hospital of Cangnan, Wenzhou Medical University, 325800 Wenzhou, Zhejiang, China
[2]Department of Dermatology, Wenzhou Central Hospital, 325000 Wenzhou, Zhejiang, China
*Correspondence: xumian4798@163.com (Mian Xu)
Submitted: 7 August 2025 Revised: 18 September 2025 Accepted: 26 September 2025 Published: 20 October 2025

Background: Atopic dermatitis (AD) is a chronic inflammatory disease characterized by immune dysregulation and skin barrier dysfunction. Recent evidence suggests that the monocyte chemotactic protein-1 (MCP-1)/C-C motif chemokine receptor 2 (CCR2) signaling pathway plays a crucial role in the recruitment of inflammatory cells and immune activation. This study aimed to investigate the role and underlying mechanisms of the MCP-1/CCR2 signaling pathway in AD pathogenesis.
Methods: A 1-Chloro-2,4-dinitrobenzene (DNCB)-induced AD mouse model and *in vitro* HaCaT cell-based experiments were employed. Clinical skin lesion scores, transepidermal water loss (TEWL), scratching bouts, and visceral indices were assessed. Histopathological changes were evaluated via hematoxylin and eosin (H&E) staining. The expression levels of inflammatory cytokines, skin barrier proteins, and components of the MCP-1/CCR2 pathway were determined using enzyme-linked immunosorbent assay (ELISA), quantitative real-time polymerase chain reaction (qRT-PCR), and Western blot analyses. Furthermore, the MCP-1/CCR2 pathway was inhibited using Bindarit to evaluate its role in modulating inflammation and barrier function.
Results: AD mice exhibited severe skin lesions, with TEWL increased by ~3.5-fold ($p < 0.05$) and scratching bouts elevated by ~3-fold ($p < 0.05$) compared to controls. Serum levels of immunoglobulin E (IgE), interleukin (IL)-4, and IL-5 were significantly higher in AD mice than in controls ($p < 0.05$). Additionally, MCP-1 and its receptor CCR2 showed time-dependent upregulation at both the mRNA and protein levels ($p < 0.05$). Following Bindarit treatment, the expression levels of inflammation-related genes were significantly reduced ($p < 0.05$), and the levels of skin barrier-associated proteins tended to normalize.
Conclusion: The MCP-1/CCR2 signaling pathway contributes to AD pathogenesis by promoting inflammatory cell recruitment and activating downstream signaling, leading to skin barrier dysfunction. Targeted inhibition of this pathway may represent a promising therapeutic strategy for alleviating AD symptoms and restoring skin barrier integrity.

Keywords: atopic dermatitis; MCP-1; *CCR2*; inflammatory response; skin barrier

Introduction

Atopic dermatitis (AD) is a common chronic inflammatory disease, affecting approximately 11%–20% of children and 5%–8% of adults. In an extensive retrospective observational study conducted in South Korea, Lee *et al.* [1] and Son *et al.* [2] identified 944,559 pediatric and 1,066,453 adult patients with AD. Clinically, AD is characterized as a heterogeneous disorder comprising various subtypes that differ according to disease stage, chronicity, age, ethnicity, and underlying molecular endotypes. The diversity among AD endotypes contributes significantly to the complexity of disease management [3]. While some conventional therapies provide adequate management for some patients, the development of innovative treatment approaches tailored to specific AD endotypes is essential to achieve optimal therapeutic outcomes.

Current treatment strategies for AD primarily focus on suppressing excessive inflammatory responses, employing agents including corticosteroids, calcineurin inhibitors, antihistamines, Janus kinase (JAK) inhibitors, and immunosuppressants [4,5]. Although these medications are clinically effective, they are often associated with specific adverse effects. For instance, topical corticosteroids may cause rebound flare-ups and, its long-term use, can lead to systemic complications [6,7]. Therefore, understanding the pathogenesis of AD and identifying key pathways that drive its inflammatory response are crucial to developing safer and more effective therapeutic strategies.

Monocyte chemotactic protein-1 (MCP-1), the ligand for C-C motif chemokine receptor 2 (CCR2), is a proinflammatory chemokine secreted by monocytes that plays a crucial role in mediating inflammatory responses [8]. Its receptor, CCR2, regulates the chemotactic activity of MCP-1 and is pivotal for the completion of the chemotaxis pro-

cess [9]. Upregulation of both MCP-1 and CCR2 has been reported in allergic dermatitis, and experimental evidence reveals that CCR2-deficient mice exhibit significantly reduced levels of inflammatory cytokines [10]. In chronic skin diseases, the aberrant activation of MCP-1 and CCR2 enhances the migration of immune cells from the bloodstream to the site of inflammation, thereby contributing to lesion formation [11]. Moreover, MCP-1 has been shown to modulate several key signaling cascades, including the NF-κB, Akt, and ERK pathways, highlighting the critical role of the MCP-1/CCR2 signaling axis in the onset and progression of inflammatory disorders [12]. Although previous studies have confirmed the upregulation of MCP-1 and CCR2 in allergic dermatitis and their role in enhancing inflammatory cell recruitment, their precise contribution to skin barrier dysfunction during AD is yet to be fully elucidated [13,14]. To our knowledge, few studies have directly addressed whether MCP-1/CCR2 signaling contributes not only to inflammatory amplification but also to structural alterations of the skin barrier [15,16].

In this study, employing both *in vivo* and *in vitro* models, we observe that MCP-1/CCR2 signaling not only enhances inflammatory responses but also aggravates skin barrier impairment in AD by modulating critical barrier-associated proteins (involucrin (IVL), loricrin (LOR), and hyaluronan synthase (HAS) family members). These findings unveil a previously unexplored mechanism and suggest that therapeutic approaches targeting the MCP-1/CCR2 pathway may offer a dual benefit, simultaneously attenuating both inflammation and barrier disruption in atopic dermatitis.

Materials and Methods

Experimental Animals

Thirty-six male BALB/c mice (specific pathogen-free (SPF) grade), aged 6 weeks and weighing 16–18 g, were purchased from Sibeifu (Beijing) Biotechnology Co., Ltd. The mice were housed under SPF conditions with a 12-hour light/dark cycle, controlled humidity and temperature, and ad libitum access to food and water. All procedures involving animals were approved by the Animal Ethics Committee of South Zhejiang Institute of Radiation Medicine and Nuclear Technology Applications (Approval No. ZFY20250116) and were conducted in accordance with institutional and international guidelines for the ethical care and use of laboratory animals.

Mice were not routinely anesthetized for topical 1-Chloro-2,4-dinitrobenzene (DNCB) application. However, for procedures likely to cause pain or substantial stress (e.g., dorsal hair removal and tissue sampling), brief anesthesia was induced with isoflurane (3–4% for induction and 1–2% for maintenance) delivered through an inhalation anesthesia system. At designated time points (Day 0, 8, 10, and 14), mice (n = 3 per group per time point) were euthanized for tissue collection. Furthermore, deep anesthesia was induced through intraperitoneal injection of pentobarbital sodium (50 mg/kg) and blood samples were collected by cardiac puncture for serum assays. For histological examination, animals were transcardially perfused with cold phosphate-buffered saline (PBS) to remove blood before excision of skin samples, which were either fixed in 4% paraformaldehyde for hematoxylin and eosin (H&E) staining or snap-frozen in liquid nitrogen for molecular analyses. After sample collection, death was confirmed by cervical dislocation. All procedures for euthanasia and terminal sampling were performed following American Veterinary Medical Association (AVMA) guidelines and institutional protocols to ensure minimal suffering.

Animal Grouping and Model Induction

After a 7-day acclimation period, BALB/c mice (n = 36) were randomly divided into three groups: blank control, AD model, and MCP-1 neutralizing antibody (NAB) groups. Dorsal hair was shaved over an area of approximately 8 cm^2 before treatment. The AD model and NAB groups were sensitized by daily topical application of 200 µL of 0.5% DNCB (Cat. No. 237329, Sigma, USA) dissolved in acetone and olive oil (3:1, v/v; acetone, Sinopharm Chemical Reagent #10000418, Shanghai, China; olive oil, Sigma-Aldrich #75343, St. Louis, MO, USA) on Days 1–3 [17,18]. From Day 8 onward, these mice were exposed to 1.0% DNCB every 3 days (Days 8, 11, and 14), for an experimental period of 14 days [19]. The blank control group received the same solvent (acetone and olive oil, 3:1, v/v) on Days 1–3 without subsequent DNCB challenge.

For intraperitoneal administration, the blank control and AD model groups were injected with 100 µL of sterile saline daily from Day 1 to Day 14. The NAB group received daily intraperitoneal injections of an anti-CCL2/JE/MCP-1 neutralizing antibody (0.2 mg/mL, R&D Systems #AF-479-NA, MN, USA) at the same volume (100 µL per mouse) over the same period [20]. On Day 0, skin samples were collected from three mice per group to establish baseline values. Furthermore, skin lesion samples were obtained from three mice per group on Days 8, 10, and 14, approximately 24 hours after the most recent treatment, and stored at –80 ºC for subsequent analyses.

Prior to sample collection, mice were anesthetized with 3% isoflurane in oxygen using an induction chamber, followed by maintenance with 1.5–2% isoflurane administered via a nose cone. After ensuring adequate anesthesia, mice were humanely euthanized by cervical dislocation in accordance with institutional ethical guidelines. Skin tissues were immediately excised, snap-frozen in liquid nitrogen, and stored at –80 °C for subsequent analysis. Tissue samples were collected at baseline (Day 0), the early inflammatory stage (Day 8), the peak of inflammation (Day 10), and the late acute inflammation phase (Day 14),

thereby enabling dynamic assessment of inflammatory and barrier-related markers.

Assessment of Skin Lesion Severity

Photographs of the dorsal skin were taken on Day 0, 8, 10, and 14. The severity of AD lesions was assessed clinically using four parameters: edema, erythema or hemorrhage, erosion or epidermal exfoliation, and crusting or dryness. Each parameter was graded on a 0–3 scale, with 0 indicating no lesion, 1 mild, 2 moderate, and 3 severe. The total dermatitis score was calculated as the sum of all parameters, ranging from 0 to 12 [18].

Trans-epidermal Water Loss (TEWL)

To evaluate skin dryness, TEWL was measured on Day 0, 8, 10, and 14 using a gpskin barrier device (GPower, Seoul, Republic of Korea). Measurements were conducted on the shaved dorsal skin center under controlled environmental conditions (21 $\pm$ 2 °C temperature and 50–55% relative humidity). The probe was applied to the skin surface for about 30 seconds until stable readings were obtained. Data were recorded as fold changes relative to controls, expressed in g/m^2·h [21].

Scratching Behavior Analysis

On Day 14, scratching behavior was recorded for 25 minutes using the Xinruan software system (Shanghai Xinruan Software Co., Ltd., Shanghai, China), and the number of hind paw scratching bouts was recorded.

Organ Index

At the end of the experiment, body weight and the weights of major organs, such as spleen, thymus, liver, lung, and kidney, were documented. The organ index was calculated using the following formula: (organ wet weight/body weight) $\times$ 100, expressed as 100 g/g.

H&E Staining

Skin lesion samples were fixed and stained using an H&E staining kit (Beyotime #C0105S, Shanghai, China). Histopathological changes were then examined under a light microscope (CX23, Olympus, Tokyo, Japan).

Enzyme-Linked Immunosorbent Assay (ELISA)

Serum samples were collected from the retro-orbital venous plexus of mice under light anesthesia with pentobarbital sodium (50 mg/kg, intraperitoneal injection) on Days 0, 8, 10, and 14 for biomarker quantification. Briefly, blood was centrifuged at 3000 rpm for 15 minutes at 4 °C, and the serum was then separated. Corresponding ELISA kits (Enzyme-linked Biotechnology, Shanghai, China) were used to measure serum levels of immunoglobulin E (IgE, #ml037602), Interleukin-4 (IL-4, #ml064310), Interleukin-5 (IL-5, #ml063157), Interleukin-1β (IL-1β, #ml106733), Interleukin-33 (IL-33, #ml063153), Interleukin-13 (IL-13, #ml106729), and Interleukin-22 (IL-22, #ml063138). Absorbance was measured at 450 nm with wavelength correction at 570 nm using a microplate reader (BioTek, Synergy H1).

Cell Culture and Stimulation

The human immortalized keratinocyte cell line HaCaT was purchased from SUNNCELL (#SNL-163, Wuhan, China) and authenticated by short tandem repeat (STR) profiling to confirm its identity and examine cross-contamination. Cells were cultured in DMEM (Thermo Fisher Scientific #12491015, Waltham, MA, USA) supplemented with 10% fetal bovine serum (Thermo Fisher Scientific #A5256701) and 1% penicillin-streptomycin (Thermo Fisher Scientific #15140122). HaCaT cells were seeded at a density of 1 $\times$ 10^5 cells/mL and incubated at 37 °C with 5% CO_2 for 24 hours. Cells between passages 5 and 15 were used for subsequent experiments. All cell cultures were routinely tested for mycoplasma contamination, and only mycoplasma-free cells were used.

Cells were divided into three groups: control, model, and Bindarit treatment (MCP-1/CCR2 signaling pathway inhibitor, MedChemExpress #130641-38-2, NJ, USA). The Bindarit group was pretreated with 100 µM Bindarit for 48 hours, followed by co-stimulation with interferon-gamma (IFN-γ, 10 ng/mL, R&D Systems #285-IF, MN, USA) and tumor necrosis factor-alpha (TNF-α, 10 ng/mL, R&D Systems #10291-TA, MN, USA) for 24 hours, consistent with the model group protocol [22].

Quantitative Real-Time Polymerase Chain Reaction (qRT-PCR)

Total RNA was extracted from mouse skin lesion tissues and human HaCaT cells using TRIzol (Thermo Fisher Scientific #15596026CN) reagent, followed by DNase I (Thermo Fisher Scientific #90083) treatment to eliminate genomic DNA contamination. One microgram of total RNA was reverse transcribed into cDNA using the High-Capacity cDNA Reverse Transcription Kit (Thermo Fisher Scientific #4368814). qRT-PCR was performed using the QuantStudio 6 Flex Real-Time PCR System (Thermo Fisher Scientific, Waltham, MA, USA) with SYBR Green detection (Thermo Fisher Scientific #11732088). Species-specific primers, such as mouse primers for mouse tissue samples and human primers for HaCaT cells, were employed. Relative mRNA expression levels were determined using the $2^{-\Delta\Delta Ct}$ method, with glyceraldehyde-3-phosphate dehydrogenase (GAPDH) as the internal control. Primer sequences used in qRT-PCR are listed in Table 1.

Western Blot Analysis

Total protein was extracted from mouse skin lesion samples and HaCaT cells using radioImmunoprecipitation assay (RIPA) lysis buffer. Protein concentrations were de-

Table 1. Primer sequences used in qRT-PCR.

Gene	Forward sequence (5′–3′)	Reverse sequence (5′–3′)	Species
Ccl2	GCTACAAGAGGATCACCAGCAG	GTCTGGACCCATTCCTTCTTGG	*Mus musculus*
CCR2	GCTGTGTTTGCCTCTCTACCAG	CAAGTAGAGGCAGGATCAGGCT	*Mus musculus*
CCL17	CGAGAGTGCTGCCTGGATTACT	GGTCTGCACAGATGAGCTTGCC	*Mus musculus*
CCL22	GTGGAAGACAGTATCTGCTGCC	AGGCTTGCGGCAGGATTTTGAG	*Mus musculus*
CCL5	CCTGCTGCTTTGCCTACCTCTC	ACACACTTGGCGGTTCCTTCGA	*Mus musculus*
IL-8	GGTGATATTCGAGACCATTTACTG	GCCAACAGTAGCCTTCACCCAT	*Mus musculus*
TSLP	GCAAATCGAGGACTGTGAGAGC	TGAGGGCTTCTCTTGTTCTCCG	*Mus musculus*
IVL	AGGAGTCACCTGAGCCAGAACT	TCAGGTGACTCCTGGTACTGCT	*Mus musculus*
LOR	ACTCCTCTCAGCAGACCAGTCA	AGAGGAGCCACCTCCACAGCT	*Mus musculus*
HAS-1	GCTACTTCCACTGTGTGTCCTG	CTAAGCATTCGGTTGGTGAGGTG	*Mus musculus*
HAS-2	CATCTGTGGAGATGGTGAAGGTC	AGCCATCCAGTATCTCACGCTG	*Mus musculus*
HAS-3	CCTTGGCAACTCAGTGGACTAC	TGGACATCTCCTCCAACACCTC	*Mus musculus*
GAPDH	CATCACTGCCACCCAGAAGACTG	ATGCCAGTGAGCTTCCCGTTCAG	*Mus musculus*
CCL17	TTCTCTGCAGCACATCCACGCA	CTGGAGCAGTCCTCAGATGTCT	*Homo sapiens*
CCL22	TCCTGGGTTCAAGCGATTCTCC	GTCAGGAGTTCAAGACCAGCCT	*Homo sapiens*
CCL5	CCTGCTGCTTTGCCTACATTGC	ACACACTTGGCGGTTCTTTCGG	*Homo sapiens*
IL-8	GAGAGTGATTGAGAGTGGACCAC	CACAACCCTCTGCACCCAGTTT	*Homo sapiens*
TSLP	TATCTGGTGCCCAGGCTATTCG	TGAAGCGACGCCACAATCCTTG	*Homo sapiens*
IVL	GGTCCAAGACATTCAACCAGCC	TCTGGACACTGCGGGTGGTTAT	*Homo sapiens*
LOR	GTCTGCGGAGGTGGTTCCTCT	TGCTGGGTCTGGTGGCAGATC	*Homo sapiens*
HAS-1	CTGGGATACTGGGTAGCCTTCA	CCAGGAACTTCTGGTTGTACCAG	*Homo sapiens*
HAS-2	ATTGTTGGCTACCAGTTTATCC	CTTTATGTGACTCATCTGTCTC	*Homo sapiens*
HAS-3	AGAGACCCCCACTAAGTACC	CAGAAGGCTGGACATATAGAG	*Homo sapiens*
GAPDH	GTCTCCTCTGACTTCAACAGCG	ACCACCCTGTTGCTGTAGCCAA	*Homo sapiens*

qRT-PCR, quantitative real-time polymerase chain reaction; *Ccl2*, C-C Motif Chemokine Ligand 2; *CCR2*, C-C motif chemokine receptor 2; *CCL*, C-C motif chemokine ligand; *IL*, interleukin; *TSLP*, thymic stromal lymphopoietin; *IVL*, involucrin; *LOR*, loricrin; *HAS*, hyaluronan synthase; *GAPDH*, glyceraldehyde-3-phosphate dehydrogenase.

termined using a bicinchoninic acid (BCA) Protein Assay Kit (Beyotime #P0012, Shanghai, China). Equal amounts of protein (20 µg) were resolved by polyacrylamide gel electrophoresis (PAGE, Thermo Fisher Scientific #89888) and subsequently transferred onto polyvinylidene fluoride (PVDF) membranes. Membranes were blocked with 5% non-fat milk (Thermo Fisher Scientific #37587) for 1 hour at room temperature, followed by overnight incubation at 4 °C with the primary antibodies listed in Table 2. The next day, the membranes were washed and then underwent a 1-hour incubation at room temperature with the appropriate horseradish peroxidase (HRP)-conjugated secondary antibodies (goat anti-rabbit immunoglobulin G (IgG), HRP, Cell Signaling Technology, #7074; goat anti-mouse IgG, HRP, CST, #7076), selected according to the host species of the primary antibody. Protein bands were then developed using enhanced chemiluminescence (ECL) reagents (Thermo Fisher Scientific #32106). These bands were visualized using the Bio-Rad ChemiDoc XRS+ imaging system (Bio-Rad, Hercules, CA, USA) and quantified with ImageJ Pro-Plus 6.0 software (Tanon, Shanghai, China).

Statistical Analysis

All statistical analyses were conducted using GraphPad Prism 7.0 software (GraphPad Software, Inc., San Diego, CA, USA). Data were presented as mean ± SEM. Data were first assessed for normality using the Shapiro-Wilk test, and homogeneity of variance was assessed using Levene's test. Outliers were identified using Grubbs' test and excluded if justified. Multiple group comparisons were performed using two-way ANOVA followed by Tukey's post hoc test for pairwise comparisons. Tukey's test was selected because it appropriately controls for family-wise error and is well-suited for balanced designs with equal group sizes. Statistical significance was indicated as follows: ns, $p > 0.05$; *$p < 0.05$; **$p < 0.01$; ***$p < 0.001$.

Results

Severity of Skin Lesions and Skin Physiological Parameters in Mice

By Day 8, mice in the AD group exhibited prominent AD-like skin lesions on the dorsal area, characterized by crusting, edema, erythema, scaling, and dryness, whereas the control group showed no obvious skin impairments. The NAB group showed intermediate symptoms, with re-

Table 2. Primary antibodies used in western blot analysis.

Antibody	Brand	Catalog number	Dilution ratio	Species
MCP-1	Abcam, Cambridge, UK	ab315478	1:1000	*Mus musculus*
CCR2	Abcam	ab273050	1:1000	*Mus musculus*
IVL	Fine Test, Wuhan, China	FNab04368	1:1000	*Mus musculus*
LOR	Fine Test	FNab04822	1:1000	*Mus musculus*
HAS-1	CUSABIO, Wuhan, China	CSB-PA547529	1:500	*Mus musculus*
HAS-2	Proteintech, Wuhan, China	83204-2-RR	1:1000	*Mus musculus*
HAS-3	Proteintech	15609-1-AP	1:1000	*Mus musculus*
IVL	Abcam	ab193353	1:1000	*Homo sapiens*
LOR	Abcam	ab176322	1:10,000	*Homo sapiens*
HAS-1	Abcam	ab198846	1:500	*Homo sapiens*
HAS-2	Abcam	ab140671	1:1000	*Homo sapiens*
HAS-3	Abcam	ab170872	1:1000	*Homo sapiens*
GAPDH	Abcam	ab8245	1:1000	Both

MCP-1, monocyte chemotactic protein-1.

duced erythema, edema, and scaling compared to the AD group, although not completely restored to control levels (Fig. 1A). Skin lesion severity scores (Fig. 1B) were significantly elevated in the AD group compared to the blank control group ($p < 0.05$). The NAB group also showed significantly higher lesion scores than the control group ($p < 0.05$); however, by Day 14, the NAB group had significantly lower lesion scores compared to the AD group ($p < 0.05$). Moreover, lesion severity in the AD group progressively increased over time relative to Day 0.

Compared with the control group, TEWL was significantly increased in the AD group ($p < 0.05$), accompanied by a significant rise in scratching bouts ($p < 0.05$, Fig. 1C,D). In the NAB group, both TEWL and scratching bouts were significantly higher than in the control group ($p < 0.05$), but substantially reduced compared with the AD group ($p < 0.05$). As shown in Fig. 1E, thymus, spleen, and lung indices were significantly elevated in the AD group compared to the controls ($p < 0.05$). No significant differences were observed in liver or kidney indices ($p > 0.05$). Conversely, the NAB group showed significantly lower thymus, spleen, and lung indices than those in the AD group ($p < 0.05$).

Histopathology of Mouse Skin Lesions

As shown in Fig. 2, the dorsal skin tissue from the blank control group exhibited normal thickness with no significant inflammatory cell infiltration. In contrast, the AD group showed pronounced epidermal thickening and edema, with evident crust formation, hyperplasia, and localized infiltration of lymphocytes and neutrophils. Compared to the AD group, mice treated with the MCP-1 neutralizing antibody exhibited reduced skin lesion thickness and decreased inflammatory cell infiltration.

Expression Levels of IgE, IL-4, IL-5, IL-1β, IL-33, IL-13, and IL-22 in Mouse Serum

The development of atopic dermatitis was associated with dynamic alterations in inflammatory cytokines (Fig. 3). Our results showed that, compared with the control group, the AD group exhibited a significant increase in serum levels of IgE, IL-1β, and IL-22 ($p < 0.05$), along with elevated levels of IL-4, IL-5, IL-33, and IL-13 ($p < 0.05$). Temporal analysis revealed that these cytokines began to rise by Day 8, reached peak levels around Day 10, and remained elevated until Day 14, consistent with the exacerbation and late stage of acute inflammation. In contrast, the NAB group showed significantly higher levels of IgE, IL-4, IL-5, IL-1β, IL-33, IL-13, and IL-22 compared with the control group ($p < 0.05$), but their levels were markedly reduced compared with the AD group ($p < 0.05$). Since MCP-1 neutralization suppressed cytokine production, this suggests that MCP-1 plays a key role in amplifying inflammatory responses during AD progression.

Expression of MCP-1 and CCR2 in Mouse Skin Lesions

Over time, both mRNA and protein levels of *MCP-1* and *CCR2* in mouse skin lesions increased progressively (Fig. 4A,B). From Day 8 onward, the expression of MCP-1 and CCR2 significantly elevated in the AD mice ($p < 0.05$). In the NAB-treated group, MCP-1 and CCR2 expression levels remained higher than in the control group ($p < 0.05$) but were substantially reduced compared with the AD group ($p < 0.05$, Fig. 4C–E).

Expression Levels of Inflammation-Related Genes in Mouse Skin Lesions

Compared to the control group, the AD group exhibited significantly elevated mRNA expression levels of inflammation-related genes, including C-C motif chemokine ligand 17 (*CCL17*), C-C motif chemokine lig-

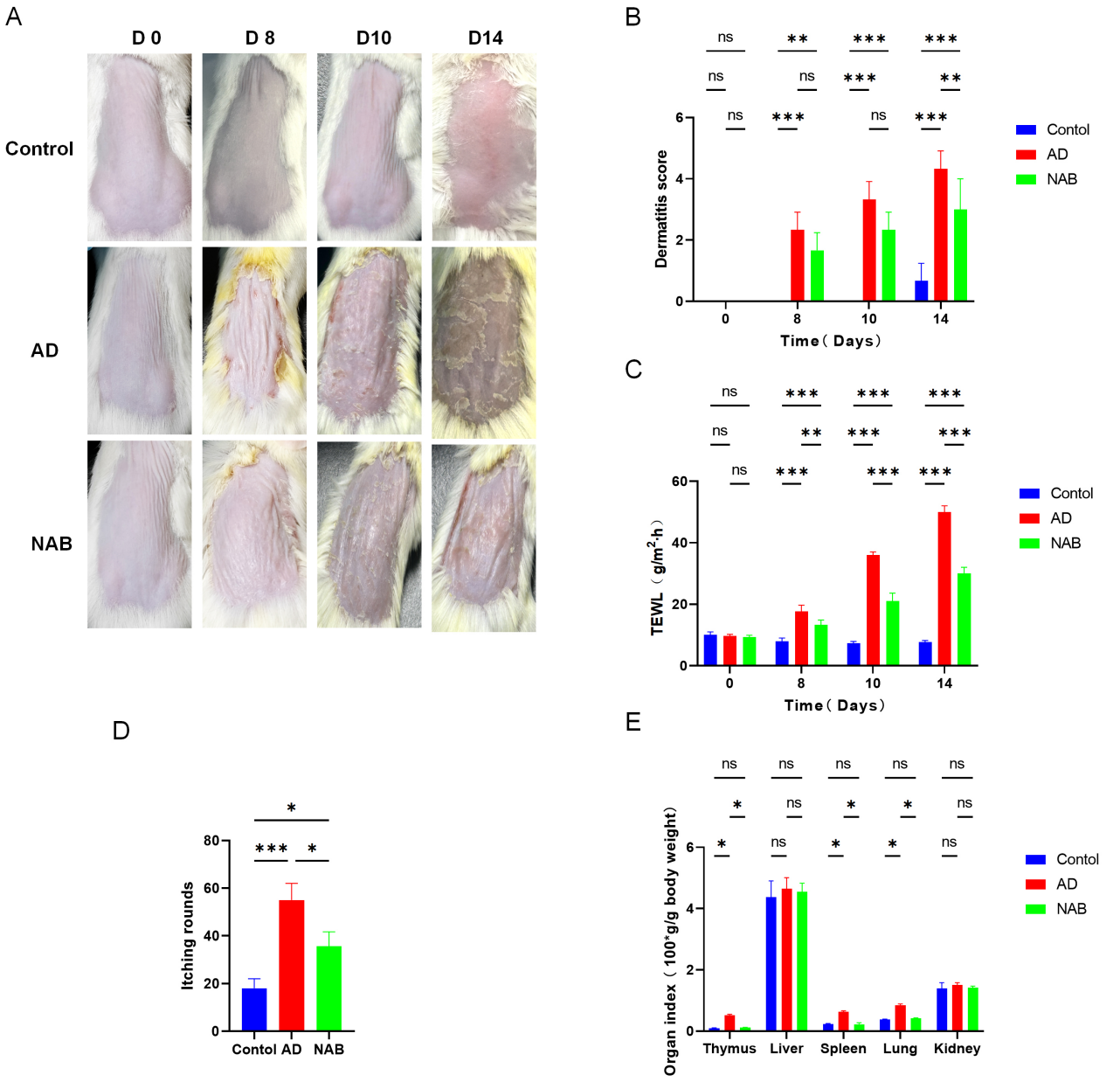

Fig. 1. Representative images of mouse skin lesions and analysis of physiological parameters. (A) Progression of skin lesions over time. (B) Dermatitis severity scores at Day 0, Day 8, Day 10, and Day 14. (C) Transepidermal water loss (TEWL) measurements. (D) Number of scratching bouts in mice. (E) Organ indices. n = 3, ***$p < 0.001$, **$p < 0.01$, *$p < 0.05$, $^{ns}p > 0.05$. AD, atopic dermatitis; NAB, neutralizing antibody.

and 22 (*CCL22*), C-C motif chemokine ligand 5 (*CCL5*), interleukin-8 (*IL-8*), and thymic stromal lymphopoietin (*TSLP*), in skin lesion tissues (Fig. 5, $p < 0.05$). The NAB group also showed higher expression of these genes than the control group ($p < 0.05$), but their levels were significantly reduced compared with the AD group ($p < 0.05$). These findings indicate that the MCP-1/CCR2 signaling pathway plays a crucial role in the inflammatory response in atopic dermatitis.

Expression Levels of Skin Barrier-Related Genes in Mouse Skin Lesions

Compared with the control group, the AD group exhibited significantly decreased mRNA expression levels of *IVL* and hyaluronan synthase 2 (*HAS-2*) in skin lesion tissues ($p < 0.05$). Conversely, the expression levels of *LOR*, hyaluronan synthase 1 (*HAS-1*), and hyaluronan synthase 3 (*HAS-3*) were significantly increased ($p < 0.05$), with protein levels showing consistent trends. In the NAB group, IVL and HAS-2 expression levels remained significantly

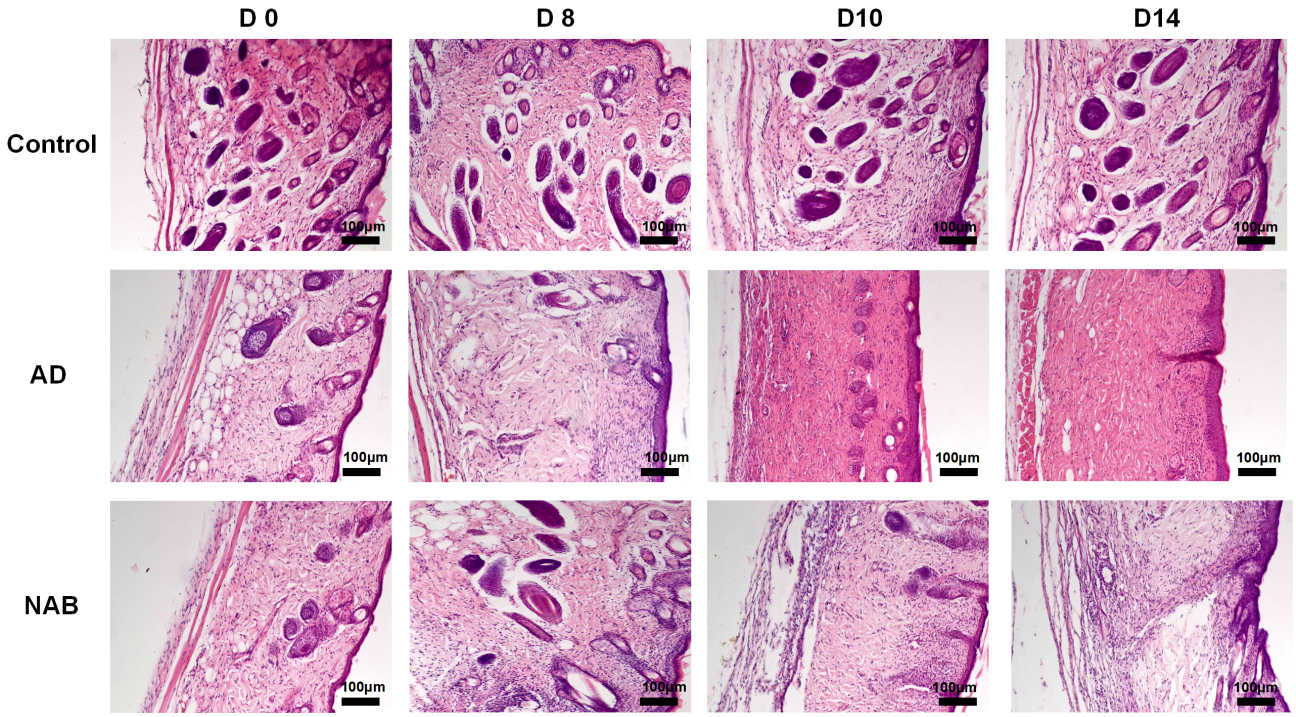

Fig. 2. Histopathological changes in mouse skin tissue. n = 3.

lower than in the control group ($p < 0.05$), whereas the expression of LOR, HAS-1, and HAS-3 was still higher ($p < 0.05$). However, compared to the AD group, IVL and HAS-2 levels were significantly upregulated ($p < 0.05$), and LOR, HAS-1, and HAS-3 were downregulated ($p < 0.05$). These observations suggest that inhibition of the MCP-1/CCR2 signaling pathway partially protects the skin barrier (Fig. 6).

Effects of MCP-1/CCR2 Signaling Pathway Inhibition on Inflammation-Related Gene Expression in HaCaT Cells

Compared to the control group, HaCaT cells in the AD model group exhibited significantly increased expression of inflammation-related genes, including *CCL17*, *CCL22*, *CCL5*, *IL-8*, and *TSLP* ($p < 0.05$), indicating that stimulation with *IFN-*γ and *TNF-*α induced their upregulation. The Bindarit-treated group also showed significantly higher expression levels of these genes compared to the control group ($p < 0.05$) but were markedly reduced relative to the AD group ($p < 0.05$). This confirms the critical role of the MCP-1/CCR2 axis in mediating the inflammatory responses *in vitro* (Fig. 7).

Expression Levels of Skin Barrier-Related Gene in HaCaT Cells After Inhibition of the MCP-1/CCR2 Signaling Pathway

As shown in Fig. 8, compared with the control group, the mRNA and protein expression levels of *IVL* and *HAS-2* were significantly decreased in the AD group ($p < 0.05$), whereas the expression levels of *LOR*, *HAS-1*, and HAS-3 were significantly increased ($p < 0.05$). After inhibition of the MCP-1/CCR2 signaling pathway, IVL and HAS-2 expression remained lower than in the control group ($p < 0.05$), while LOR, HAS-1, and HAS-3 were significantly higher ($p < 0.05$). However, compared to the AD group, Bindarit treatment substantially upregulated IVL and HAS-2 expression levels ($p < 0.05$) and significantly downregulated LOR, HAS-1, and HAS-3 ($p < 0.05$). These results further confirm that during the progression of AD, the MCP-1/CCR2 signaling pathway accelerates the disruption of the skin's physical barrier.

Discussion

Inflammatory Mechanisms in AD

AD is a common inflammatory skin disorder characterized primarily by pruritus, which often worsens at night, along with dry, thickened, and lichenified skin presenting with intensely itchy papules. Persistent scratching often leads to excoriation and bleeding [23,24]. The development of AD is strongly associated with skin barrier dysfunction and inflammatory mechanisms [25]. During AD flare-ups, TSLP activates dendritic cells, resulting in elevated levels of inflammatory cytokines, including IL-4, IL-5, IL-22, and IL-13. This cascade enhances the excessive release of IgE from plasma cells and an increase in eosinophil numbers, thereby triggering inflammatory responses [26].

In this study, a DNCB-induced AD mouse model was established to systematically investigate the role of

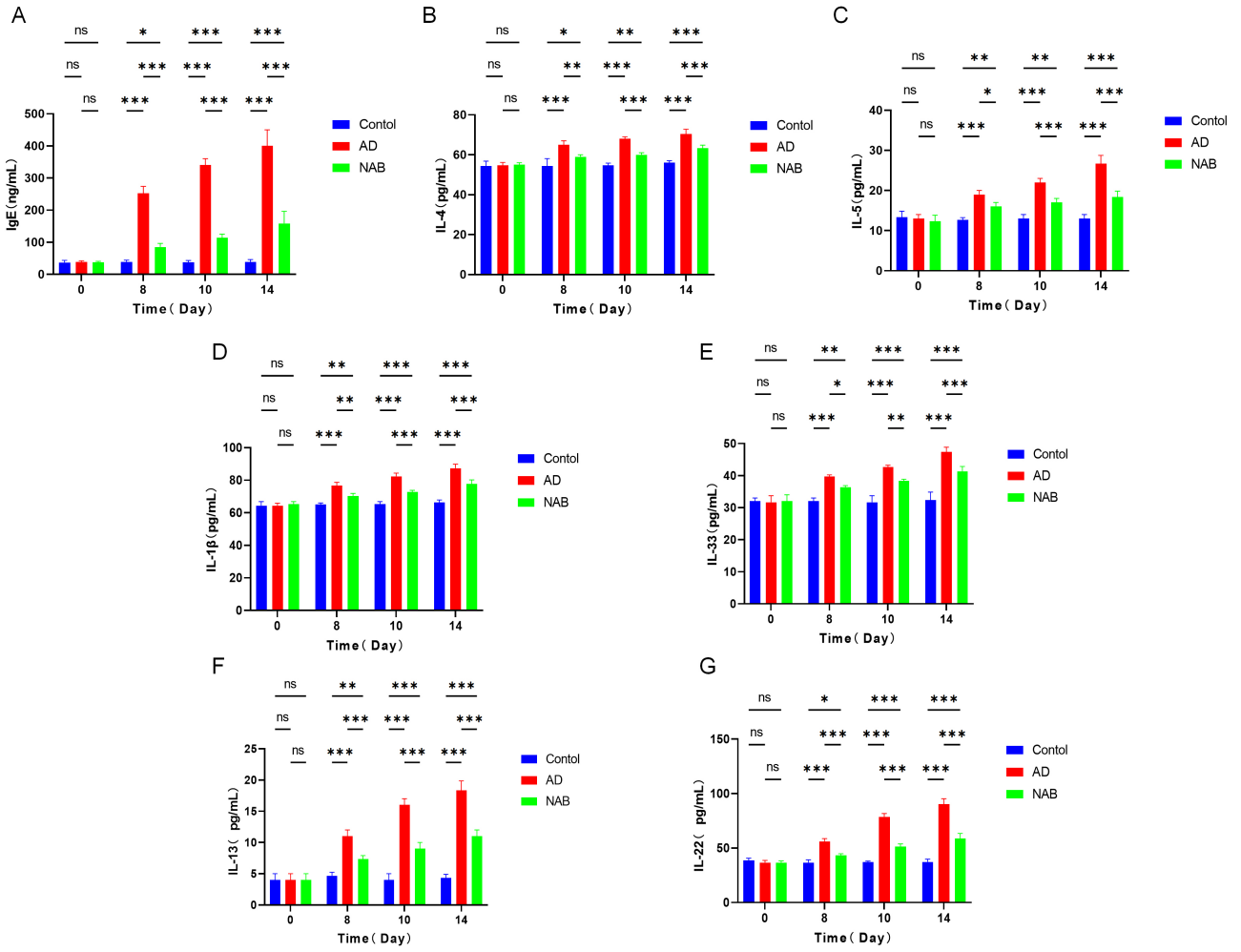

Fig. 3. Levels of inflammatory cytokines in mouse serum. (A) Immunoglobulin E (IgE). (B) IL-4. (C) IL-5. (D) IL-1β. (E) IL-33. (F) IL-13. (G) IL-22. n = 3, ***$p < 0.001$, **$p < 0.01$, *$p < 0.05$, $^{ns}p > 0.05$.

MCP-1 and its receptor CCR2 in AD pathogenesis. AD mice displayed evident skin lesions (Fig. 1A,B), increased transepidermal water loss (Fig. 1C), and substantially elevated serum cytokine levels (Fig. 3) compared with controls. Importantly, blocking the MCP-1/CCR2 pathway using a neutralizing antibody significantly improved skin lesions (Fig. 1A), alleviated barrier impairment (Fig. 2), and decreased both serum cytokine levels and inflammatory gene expression in skin tissues (Figs. 3,4). These findings highlight the crucial role of MCP-1/CCR2 signaling in driving and amplifying inflammatory responses in AD.

MCP-1, a key pro-inflammatory chemokine, is substantially upregulated during inflammatory responses and recruits monocytes and other inflammatory cells to sites of skin injury, thereby exacerbating the local inflammatory response [27,28]. CCR2, the primary receptor for MCP-1, activates downstream signaling cascades, including *NF-κB*, *Akt*, and *ERK*, further promoting cytokine production [29–31]. Our results revealed time-dependent upregulation of MCP-1 and CCR2 expression in AD lesions (Figs. 4,5), which correlated with worsening skin damage and increased cytokine levels, highlighting their central role in mediating the inflammatory cascade.

Barrier Disruption and Hyaluronan Metabolism

Beyond its role in inflammation, MCP-1/CCR2 signaling was closely linked to skin barrier disruption. Interestingly, we observed upregulation of *HAS-1* and *HAS-3*, along with downregulation of *HAS-2* (Fig. 6). This pattern is consistent with previous studies demonstrating that *HAS-1* and *HAS-3* generate low-molecular-weight hyaluronan fragments with pro-inflammatory activity, whereas *HAS-2* primarily produces high-molecular-weight hyaluronan, which exerts anti-inflammatory and barrier-stabilizing effects [32,33]. These findings suggest that MCP-1/CCR2 signaling may disrupt hyaluronan homeostasis, thereby amplifying inflammation while compromising barrier integrity.

In HaCaT cells, AD-like conditions reduced *IVL* and *HAS-2* expression levels, but increased *LOR*, *HAS-1*, and

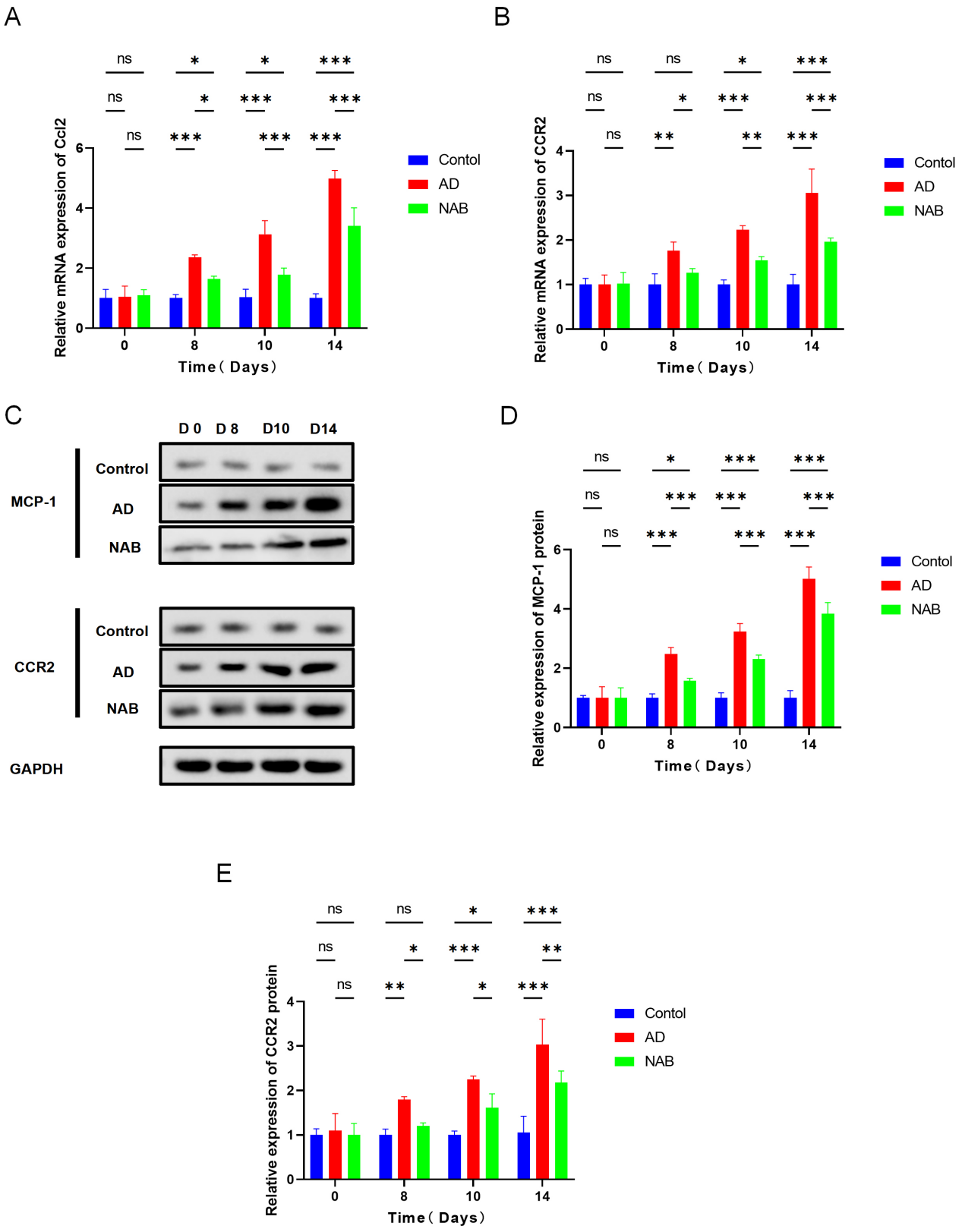

Fig. 4. Expression levels of *Ccl2* and *CCR2* in mouse skin lesion tissues. (A) *Ccl2* mRNA levels. (B) *CCR2* mRNA levels. (C–E) Western blot analysis and quantification of MCP-1 and CCR2 protein expression. n = 3, ***$p < 0.001$, **$p < 0.01$, *$p < 0.05$, $^{ns}p > 0.05$.

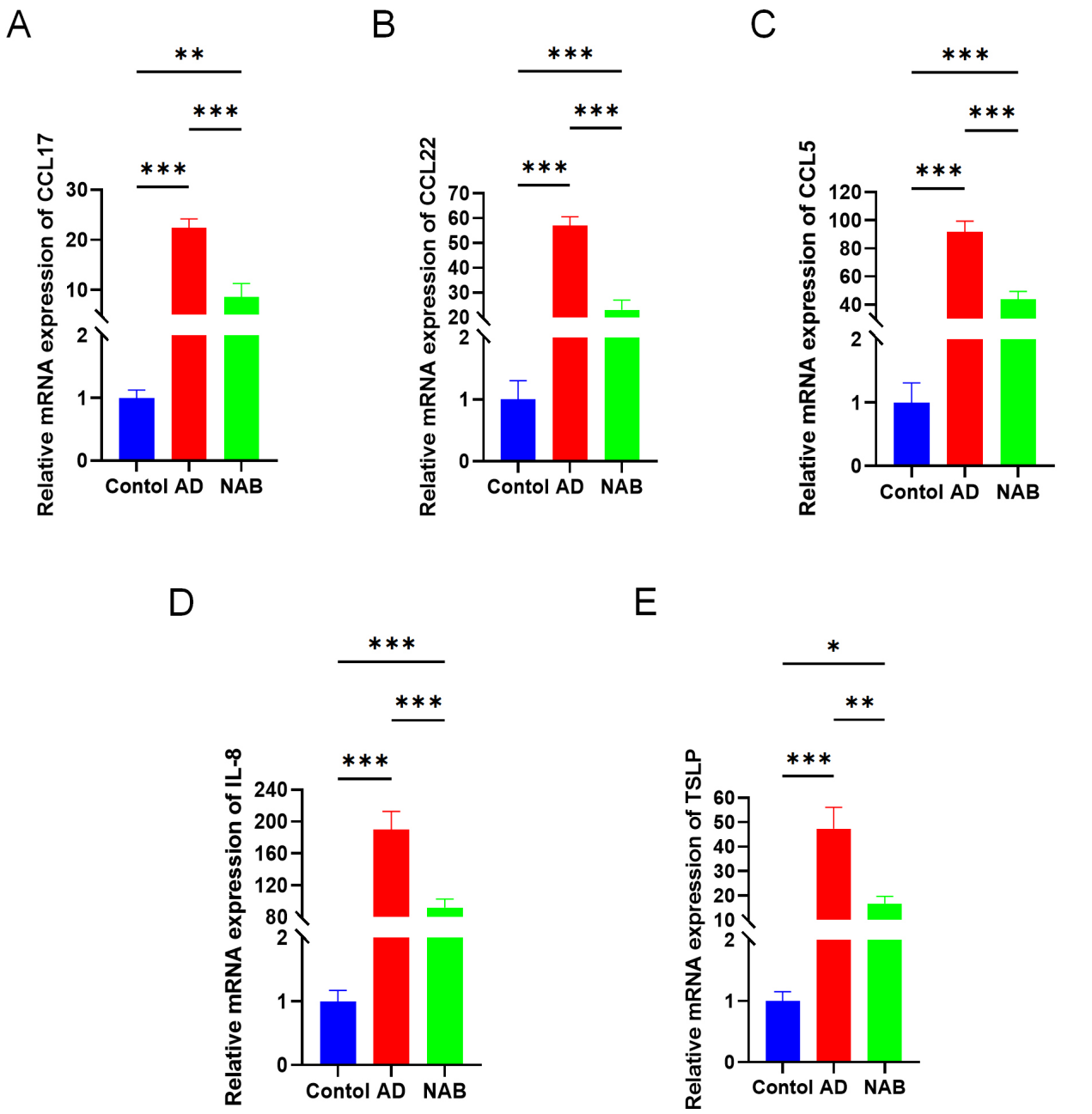

Fig. 5. Expression levels of inflammation-related genes in mouse skin lesion tissues. (A–E) Relative mRNA expression levels of CCL17, CCL22, CCL5, IL-8, and TSLP in mouse skin lesion tissues were determined using qRT-PCR. n = 3, ***$p < 0.001$, **$p < 0.01$, *$p < 0.05$.

HAS-3 expression, indicating that MCP-1/CCR2 pathway regulates keratinocyte differentiation and barrier protein expression (Fig. 8). This finding aligns with previous evidence linking abnormalities in stratum corneum lipids and lamellar bodies to barrier dysfunction [34]. Thus, this confirms that MCP-1/CCR2 signaling contributes to a vicious cycle in which persistent inflammation further aggravates barrier damage.

Therapeutic Significance of MCP-1/CCR2 Inhibition

Despite different intervention strategies being applied *in vivo* and *in vitro*, both antibody blockade in mice (Figs. 1,2,3,4,5,6) and Bindarit treatment in HaCaT cells (Figs. 7,8) consistently suppressed MCP-1/CCR2 activity. *In vivo*, inhibition reduced AD lesions, serum cytokines, and organ indices, while suppressing inflammation-related genes (*CCL17*, *CCL22*, *CCL5*, *IL-8*, *TSLP*) and partially restoring barrier proteins *in vitro* (Fig. 8). This complementary experimental design confirms that MCP-1/CCR2

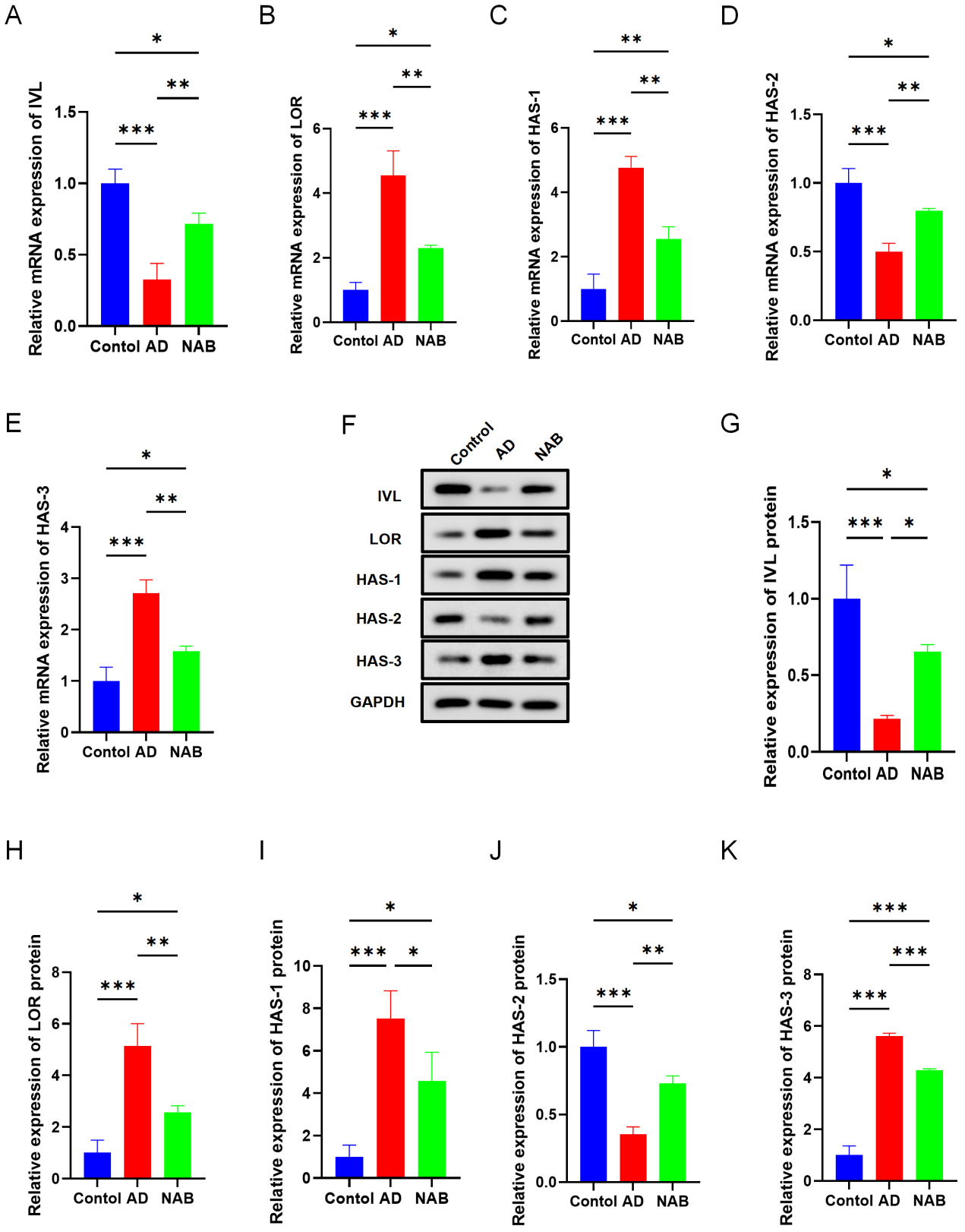

Fig. 6. Expression levels of skin barrier-related genes in mouse skin lesion tissues. (A–E) mRNA expression levels of *IVL*, *LOR*, *HAS-1*, *HAS-2*, and *HAS-3*. (F–K) Western blot analysis and quantification of IVL, LOR, HAS-1, HAS-2, and HAS-3 protein expression. n = 3, ***$p < 0.001$, **$p < 0.01$, *$p < 0.05$.

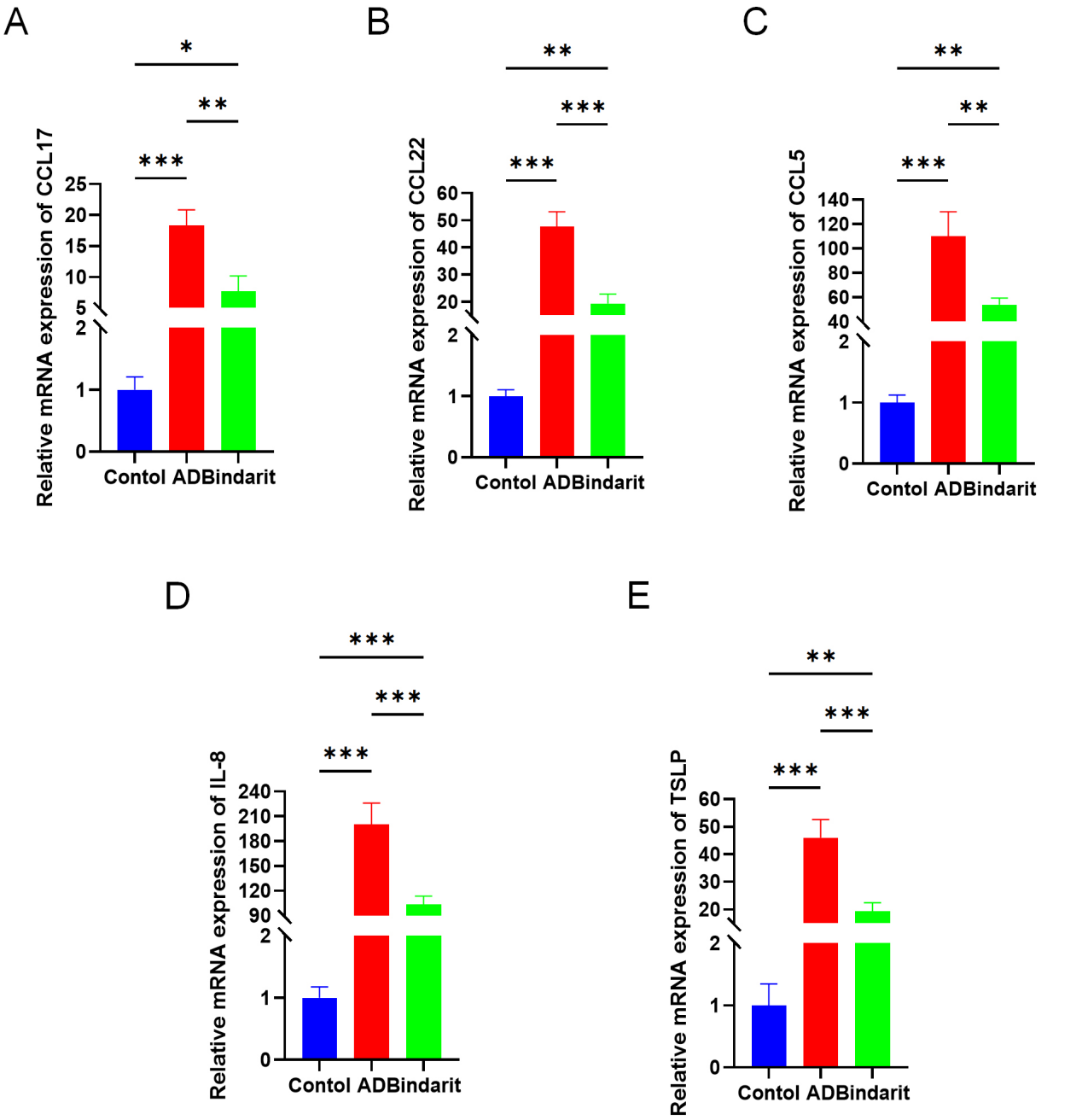

Fig. 7. Expression levels of inflammation-related genes in HaCaT cells. (A–E) Relative mRNA expression levels of CCL17, CCL22, CCL5, IL-8, and TSLP in HaCaT cells were assessed using qRT-PCR. n = 3, ***$p < 0.001$, **$p < 0.01$, *$p < 0.05$.

signaling is a pivotal driver of both inflammation and barrier dysfunction. Previous studies have also revealed that anti-inflammatory therapies can enhance barrier repair by reducing inflammatory cell infiltration and cytokine levels, limiting epidermal hyperplasia, and accelerating tissue recovery [33,35,36]. Together, these findings underscore the therapeutic potential of MCP-1/CCR2 inhibitors in AD management.

To summarize our findings, a schematic diagram is provided in Fig. 9, outlining the proposed mechanism by which MCP-1/CCR2 signaling exacerbates AD pathology through amplification of inflammation, downregulation of barrier protein, and altered expression of HAS isoform.

Novelty and Limitations

This study substantiates the critical role of MCP-1/CCR2 signaling in AD pathogenesis, highlighting its dual contribution to cytokine secretion and barrier impairment. A key novelty lies in elucidating its involvement in hyaluronan dysregulation and keratinocyte differentiation, thereby

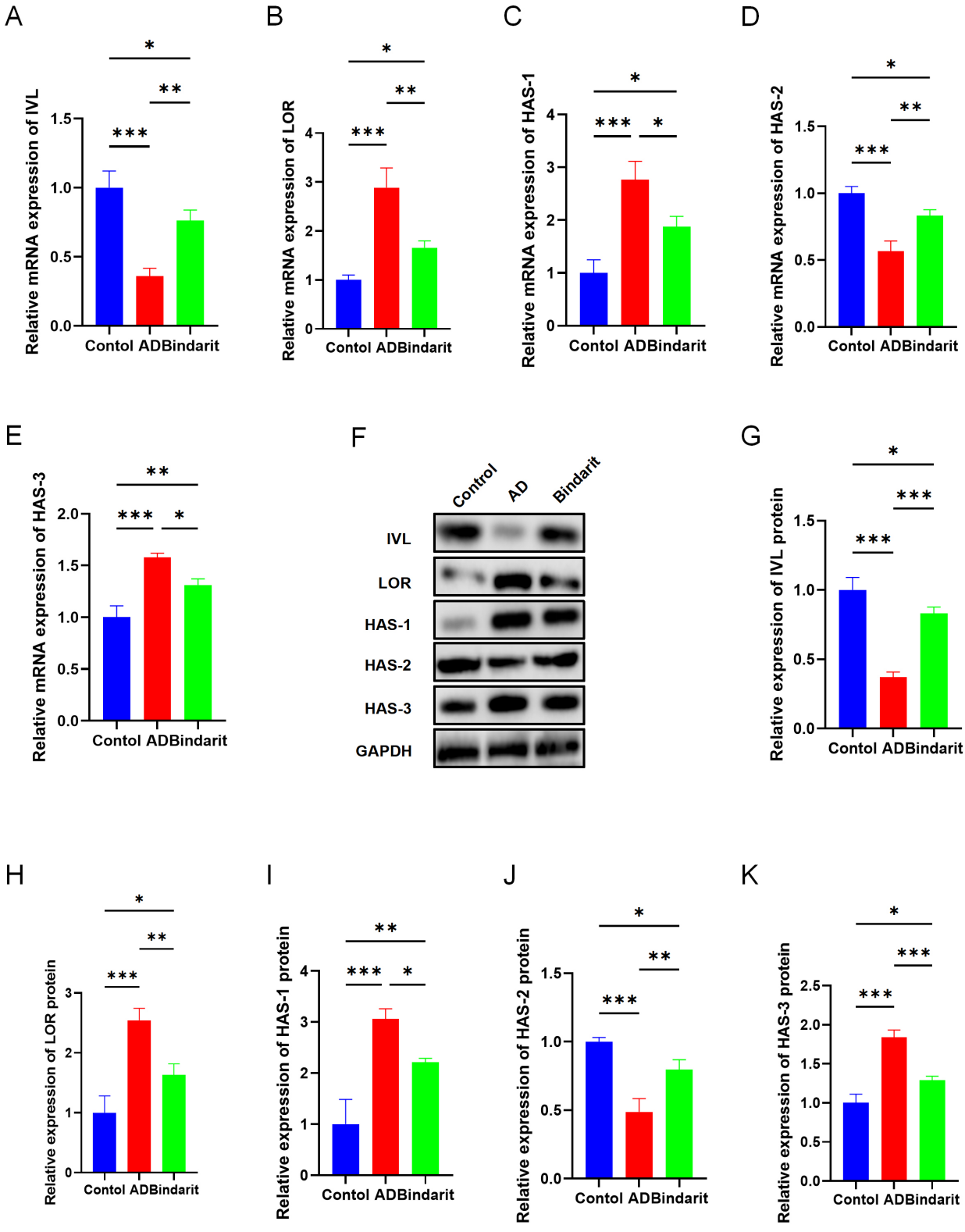

Fig. 8. Expression levels of skin barrier-related genes in HaCaT cells. (A–E) mRNA expression levels of *IVL*, *LOR*, *HAS-1*, *HAS-2*, and *HAS-3*. (F–K) Western blot analysis and quantification of protein expression levels of IVL, LOR, HAS-1, HAS-2, and HAS-3. n = 3, ***$p < 0.001$, **$p < 0.01$, *$p < 0.05$.

providing a molecular rationale for targeted interventions [37–39]. Nevertheless, certain limitations should be acknowledged. The DNCB-induced model only partially reflects the clinical heterogeneity of AD, and HaCaT cell

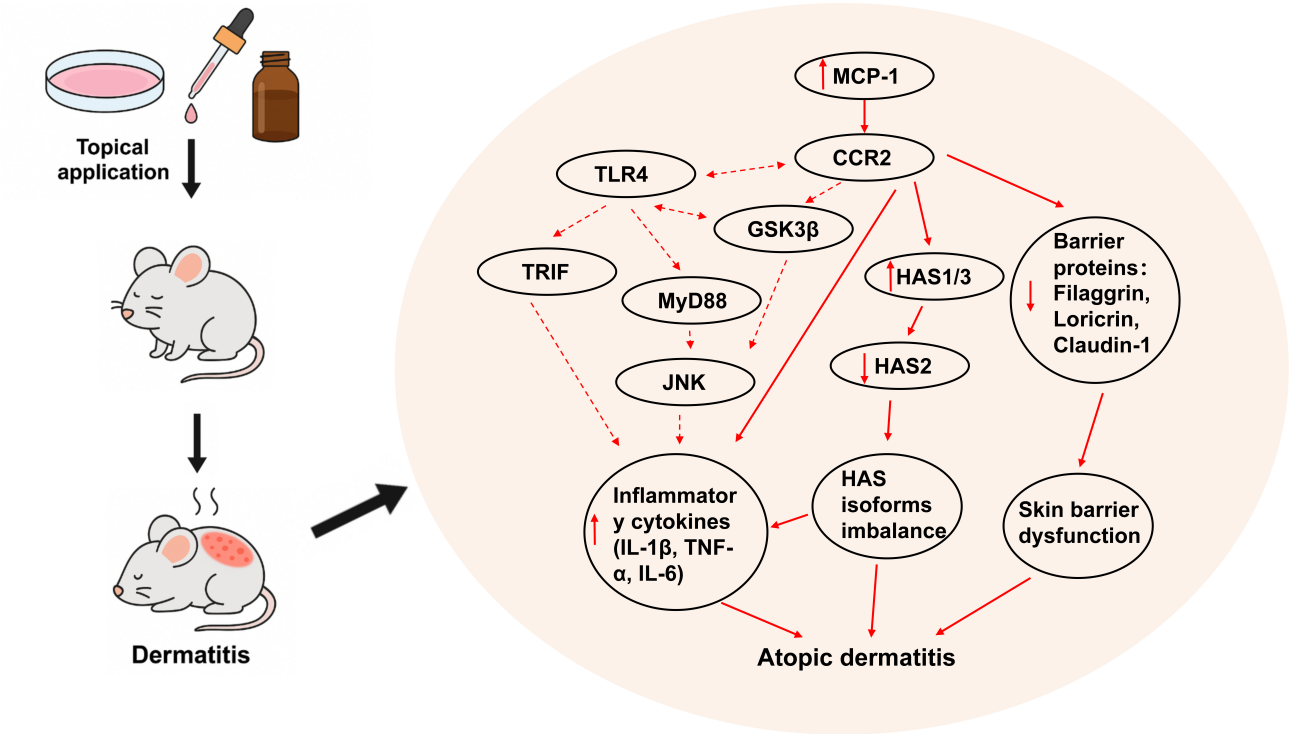

Fig. 9. Proposed mechanism of MCP-1/CCR2 signaling in atopic dermatitis. The dashed lines represent mechanisms that were not investigated in the present study. ↑ and ↓ indicate upregulation and downregulation of the corresponding genes, respectively. TLR4, toll-Like receptor 4; GSK3β, glycogen synthase kinase 3 beta; TRIF, TIR-domain-containing adapter-inducing interferon-β; MyD88, myeloid differentiation primary response 88; JNK, c-Jun N-terminal kinase; TNF-α, tumor necrosis factor-alpha.

assays cannot fully replicate *in vivo* complexity. Future studies should incorporate additional experimental models, larger cohorts, and clinical samples, while also investigating crosstalk between MCP-1/CCR2 and other cytokine networks. Another limitation is that the downstream signaling pathways, such as those involving phosphorylated NF-κB or Akt, were not evaluated in this study. Future studies should include analysis of these pathways to clarify the mechanistic links between MCP-1/CCR2 activation, inflammatory amplification, and barrier disruption.

Conclusion

In summary, this study demonstrates that MCP-1/CCR2 signaling promotes inflammatory cell chemotaxis, activates pro-inflammatory pathways, and disrupts barrier integrity, thereby driving AD pathogenesis. Targeting this pathway may offer a promising therapeutic strategy, warranting future validation in preclinical and clinical studies.

Abbreviations

AD, atopic dermatitis; MCP-1, monocyte chemotactic protein-1; CCR2, C-C motif chemokine receptor 2; NAB, neutralizing antibody; DNCB, 1-chloro-2,4-dinitrobenzene; TEWL, transepidermal water loss; H&E, hematoxylin and eosin; ELISA, enzyme-linked immunosorbent assay; qRT-PCR, quantitative real-time polymerase chain reaction; IFN-γ, interferon-gamma; TNF-α, tumor necrosis factor-alpha; IVL, involucrin; LOR, loricrin; HAS-1, hyaluronan synthase 1; HAS-2, hyaluronan synthase 2; HAS-3, hyaluronan synthase 3; TSLP, thymic stromal lymphopoietin; IgE, immunoglobulin E.

Availability of Data and Materials

The data that support the findings of this study are available from the corresponding author upon reasonable request.

Author Contributions

JC and MX designed the research study. JC performed the research. JC and MX collected and analyzed the data. JC and MX have been involved in drafting the manuscript and both authors have been involved in revising it critically for important intellectual content. Both authors give final approval of the version to be published. Both authors have participated sufficiently in the work to take public responsibility for appropriate portions of the content and agreed to be accountable for all aspects of the work in ensuring that questions related to its accuracy or integrity are appropriately investigated and resolved.

Ethics Approval and Consent to Participate

All animal experiments were approved by the Animal Ethics Committee of South Zhejiang Institute of Radiation Medicine and Nuclear Technology Applications (Approval No. ZFY20250116).

Acknowledgment

Not applicable.

Funding

This research received no external funding.

Conflict of Interest

The authors declare no conflict of interest.

References

[1] Lee JH, Choi A, Noh Y, Oh IS, Jeon JY, Yoo HJ, *et al*. Real-world treatment patterns for atopic dermatitis in South Korea. Scientific Reports. 2022; 12: 13626. https://doi.org/10.1038/s41598-022-17222-y.

[2] Son SW, Lee JH, Ahn J, Chang SE, Choi EH, Han TY, *et al*. Assessment of Disease Severity and Quality of Life in Patients with Atopic Dermatitis from South Korea. Annals of Dermatology. 2022; 34: 419–430. https://doi.org/10.5021/ad.21.239.

[3] Tokura Y, Hayano S. Subtypes of atopic dermatitis: From phenotype to endotype. Allergology International: Official Journal of the Japanese Society of Allergology. 2022; 71: 14–24. https://doi.org/10.1016/j.alit.2021.07.003.

[4] Bieber T. Atopic dermatitis: an expanding therapeutic pipeline for a complex disease. Nature Reviews. Drug Discovery. 2022; 21: 21–40. https://doi.org/10.1038/s41573-021-00266-6.

[5] Naik PP. Treatment-resistant atopic dermatitis: novel therapeutics, digital tools, and precision medicine. Asia Pacific Allergy. 2022; 12: e20. https://doi.org/10.5415/apallergy.2022.12.e20.

[6] Hengge UR, Ruzicka T, Schwartz RA, Cork MJ. Adverse effects of topical glucocorticosteroids. Journal of the American Academy of Dermatology. 2006; 54: 1–1–15; quiz 16–18. https://doi.org/10.1016/j.jaad.2005.01.010.

[7] Obed O, Chong AC, Su M, Ong PY. Emerging drugs for the treatment of atopic dermatitis: a focus on phase 2 and phase 3 trials. Expert Opinion on Emerging Drugs. 2024; 29: 233–249. https://doi.org/10.1080/14728214.2024.2345643.

[8] Hu X, Zhao W, Deng J, Du Z, Zeng X, Zhou B, *et al*. Mangiferin alleviates renal inflammatory injury in spontaneously hypertensive rats by inhibiting MCP-1/CCR2 signaling pathway. Chinese Herbal Medicines. 2023; 15: 556–563. https://doi.org/10.1016/j.chmed.2022.12.008.

[9] Ou X, Wen T, Ying J, He Q, Xuan A, Ruan D. MCP 1/CCR2 axis inhibits the chondrogenic differentiation of human nucleus pulposus mesenchymal stem cells. Molecular Medicine Reports. 2022; 26: 277. https://doi.org/10.3892/mmr.2022.12793.

[10] Shibuya R, Ishida Y, Hanakawa S, Kataoka TR, Takeuchi Y, Murata T, *et al*. CCL2–CCR2 Signaling in the Skin Drives Surfactant-Induced Irritant Contact Dermatitis through IL-1β–Mediated Neutrophil Accumulation. The Journal of Investigative Dermatology. 2022; 142: 571–582.e9. https://doi.org/10.1016/j.jid.2021.07.182.

[11] Behfar S, Hassanshahi G, Nazari A, Khorramdelazad H. A brief look at the role of monocyte chemoattractant protein-1 (CCL2) in the pathophysiology of psoriasis. Cytokine. 2018; 110: 226–231. https://doi.org/10.1016/j.cyto.2017.12.010.

[12] Singh S, Anshita D, Ravichandiran V. MCP-1: Function, regulation, and involvement in disease. International Immunopharmacology. 2021; 101: 107598. https://doi.org/10.1016/j.intimp.2021.107598.

[13] Vestergaard C, Just H, Baumgartner Nielsen J, Thestrup-Pedersen K, Deleuran M. Expression of CCR2 on monocytes and macrophages in chronically inflamed skin in atopic dermatitis and psoriasis. Acta Dermato-venereologica. 2004; 84: 353–358. https://doi.org/10.1080/00015550410034444.

[14] Wang H, Li H, Li Z, Zhao X, Hou X, Chen L, *et al*. Crisaborole combined with vitamin D demonstrates superior therapeutic efficacy over either monotherapy in mice with allergic contact dermatitis. Scientific Reports. 2024; 14: 20092. https://doi.org/10.1038/s41598-024-71135-6.

[15] Son Y, Yang W, Park S, Yang J, Kim S, Lyu JH, *et al*. The Anti-Inflammatory and Skin Barrier Function Recovery Effects of *Schisandra chinensis* in Mice with Atopic Dermatitis. Medicina (Kaunas, Lithuania). 2023; 59: 1353. https://doi.org/10.3390/medicina59071353.

[16] Yamamura Y, Nakashima C, Otsuka A. Interplay of cytokines in the pathophysiology of atopic dermatitis: insights from Murin models and human. Frontiers in Medicine. 2024; 11: 1342176. https://doi.org/10.3389/fmed.2024.1342176.

[17] Han SY, Im DS. Evodiamine Alleviates 2,4-Dinitro-1-Chloro-Benzene-Induced Atopic Dermatitis-like Symptoms in BALB/c Mice. Life (Basel, Switzerland). 2024; 14: 494. https://doi.org/10.3390/life14040494.

[18] Riedl R, Kühn A, Hupfer Y, Hebecker B, Peltner LK, Jordan PM, *et al*. Characterization of Different Inflammatory Skin Conditions in a Mouse Model of DNCB-Induced Atopic Dermatitis. Inflammation. 2024; 47: 771–788. https://doi.org/10.1007/s10753-023-01943-x.

[19] Jeong M, Kwon H, Kim Y, Jin H, Choi GE, Hyun KY. *Erigeron annuus* Extract Improves DNCB-Induced Atopic Dermatitis in a Mouse Model via the Nrf2/HO-1 Pathway. Nutrients. 2024; 16: 451. https://doi.org/10.3390/nu16030451.

[20] Suresh MV, Yalamanchili G, Rao TC, Aktay S, Kralovich A, Shah YM, *et al*. Hypoxia-inducible factor (HIF)-1α-induced regulation of lung injury in pulmonary aspiration is mediated through NF-kB. FASEB BioAdvances. 2022; 4: 309–328. https://doi.org/10.1096/fba.2021-00132.

[21] Yun HR, Ahn SW, Seol B, Vasileva EA, Mishchenko NP, Fedoreyev SA, *et al*. Echinochrome A Treatment Alleviates Atopic Dermatitis-like Skin Lesions in NC/Nga Mice via IL-4 and IL-13 Suppression. Marine Drugs. 2021; 19: 622. https://doi.org/10.3390/md19110622.

[22] Zeng Y, Nie X, Deng Y. CCL19 promotes TNF-alpha/IFN-gamma-induced production of cytokines by targeting CCR7/NF-κB signalling in HaCaT cells. Folia Histochemica et Cytobiologica. 2024; 62: 203–211. https://doi.org/10.5603/fhc.104038.

[23] Ahn C, Huang W. Clinical Presentation of Atopic Dermatitis. Advances in Experimental Medicine and Biology. 2024; 1447: 37–44. https://doi.org/10.1007/978-3-031-54513-9_4.

[24] Zhang L, Chen N, Liao Y, Kong Y, Yang X, Zhan M, *et al*. Efficacy and action mechanisms of compound Shen Chan decoction on experimental models of atopic dermatitis. International Immunopharmacology. 2024; 137: 112479. https://doi.org/10.1016/j.intimp.2024.112479.

[25] Yamamura K, Ohno F, Yotsumoto S, Sato Y, Kimura N, Nishio K, *et al*. Extracellular ATP Contributes to Barrier Function and Inflammation in Atopic Dermatitis: Potential for Topical Treatment of Atopic Dermatitis by Targeting Extracellular ATP. International Journal of Molecular Sciences. 2024; 25: 12294. https://doi.org/10.3390/ijms252212294.

[26] Sroka-Tomaszewska J, Trzeciak M. Molecular Mechanisms of Atopic Dermatitis Pathogenesis. International Journal of Molecular Sciences. 2021; 22: 4130. https://doi.org/10.3390/ijms22084130.

[27] Tian S, Chen X, Wu W, Lin H, Qing X, Liu S, *et al*. Nucleus pulposus cells regulate macrophages in degenerated intervertebral discs via the integrated stress response-mediated CCL2/7-CCR2 signaling pathway. Experimental & Molecular Medicine. 2024; 56: 408–421. https://doi.org/10.1038/s12276-024-01168-4.

[28] Liu Y, Xu K, Xiang Y, Ma B, Li H, Li Y, *et al*. Role of MCP-1 as an inflammatory biomarker in nephropathy. Frontiers in Immunology. 2024; 14: 1303076. https://doi.org/10.3389/fimmu.2023.1303076.

[29] Mei C, Meng F, Wang X, Yan S, Zheng Q, Zhang X, *et al*. CD30L is involved in the regulation of the inflammatory response through inducing homing and differentiation of monocytes via CCL2/CCR2 axis and NF-κB pathway in mice with colitis. International Immunopharmacology. 2022; 110: 108934. https://doi.org/10.1016/j.intimp.2022.108934.

[30] Guo S, Zhang Q, Guo Y, Yin X, Zhang P, Mao T, *et al*. The role and therapeutic targeting of the CCL2/CCR2 signaling axis in inflammatory and fibrotic diseases. Frontiers in Immunology. 2025; 15: 1497026. https://doi.org/10.3389/fimmu.2024.1497026.

[31] Song N, Cui K, Zeng L, Li M, Fan Y, Shi P, *et al*. Advance in the role of chemokines/chemokine receptors in carcinogenesis: Focus on pancreatic cancer. European Journal of Pharmacology. 2024; 967: 176357. https://doi.org/10.1016/j.ejphar.2024.176357.

[32] Schmuth M, Eckmann S, Moosbrugger-Martinz V, Ortner-Tobider D, Blunder S, Trafoier T, *et al*. Skin Barrier in Atopic Dermatitis. The Journal of Investigative Dermatology. 2024; 144: 989–1000.e1. https://doi.org/10.1016/j.jid.2024.03.006.

[33] van den Bogaard EH, Elias PM, Goleva E, Berdyshev E, Smits JPH, Danby SG, *et al*. Targeting Skin Barrier Function in Atopic Dermatitis. The Journal of Allergy and Clinical Immunology. in Practice. 2023; 11: 1335–1346. https://doi.org/10.1016/j.jaip.2023.02.005.

[34] Mahanty S. Skin lamellar bodies: a unique set of lysosome-related organelles. Frontiers in Cell and Developmental Biology. 2025; 13: 1597696. https://doi.org/10.3389/fcell.2025.1597696.

[35] Montero-Vilchez T, Rodriguez-Pozo JA, Diaz-Calvillo P, Salazar-Nievas M, Tercedor-Sanchez J, Molina-Leyva A, *et al*. Dupilumab Improves Skin Barrier Function in Adults with Atopic Dermatitis: A Prospective Observational Study. Journal of Clinical Medicine. 2022; 11: 3341. https://doi.org/10.3390/jcm11123341.

[36] Rohner MH, Thormann K, Cazzaniga S, Yousefi S, Simon HU, Schlapbach C, *et al*. Dupilumab reduces inflammation and restores the skin barrier in patients with atopic dermatitis. Allergy. 2021; 76: 1268–1270. https://doi.org/10.1111/all.14664.

[37] Alam MJ, Xie L, Yap YA, Robert R. A Mouse Model of MC903-Induced Atopic Dermatitis. Current Protocols. 2023; 3: e695. https://doi.org/10.1002/cpz1.695.

[38] Guttman-Yassky E, Renert-Yuval Y, Brunner PM. Atopic dermatitis. Lancet (London, England). 2025; 405: 583–596. https://doi.org/10.1016/S0140-6736(24)02519-4.

[39] Napolitano M, Esposito M, Fargnoli MC, Girolomoni G, Romita P, Nicoli E, *et al*. Infections in Patients with Atopic Dermatitis and the Influence of Treatment. American Journal of Clinical Dermatology. 2025; 26: 183–197. https://doi.org/10.1007/s40257-025-00917-z.